ISSN 1027-5495. Functional Materials, 28, No.2 (2021), p. 221-224.
doi:https://doi.org/10.15407/fm28.02.221

Study of hydrothermal synthesis of $NiFe_2O_4$ on morphology, crystallinity, chemical and magnetic properties

Marhaposan Situmorang, Perdinan Sinuhaji, Muhammadin Hamid, Nurul Yaumilda Hasibuan, Martha Rianna

Department of Physics, Universitas Sumatera Utara, 20155 Medan, Indonesia

Received February 3, 2021

In this work, spinel ferrite $NiFe_2O_4$ was synthesized using the low temperature hydrothermal method with various ratios between $Ni(NO_3)_2$ and $FeCl_2$, namely, 1:1, 1:2, 2:1 and 2:3, followed by annealing process at 300°C for 1 h. Based on analysis with a scanning electron microscope , we found that nanosheets were formed at low Ni ratio; however at a higher ratio, $FeCl_2$, nanoparticles are present. In addition, X-ray diffraction revealed the crystallinity of $NiFe_2O_4$ with a crystalline size of approximately 15 nm. Besides, Fourier transform infrared spectroscopy explained the chemical properties of $NiFe_2O_4$ by Fe–O vibrations. Furthermore, the vibrating sample magnetometer demonstrated excellent magnetic properties of $NiFe_2O_4$, which correlated with high crystallinity of $NiFe_2O_4$ nanosheets.

Keywords: spinel ferrite, hydrothermal synthesis, magnetic properties.

Дослідження морфології, кристалічності, хімічних та магнітних властивостей **$NiFe_2O_4$, синтезованого гідротермальним методом.** *Marhaposan Situmorang, Perdinan Sinuhaji, Muhammadin Hamid, Nurul Yaumilda Hasibuan, Martha Rianna*

Ферит шпінелі $NiFe_2O_4$ синтезовано низькотемпературним гідротермальним методом з різним співвідношенням $Ni(NO_3)_2$ і $FeCl_2$, а саме 1:1, 1:2, 2:1 і 2:3, з подальшим відпалом при температурі 300°C протягом 1 г. Виявлено, що формування нанопластин відбувається при низькому вмісті Ni і при більш високому вмісті $FeCl_2$. Розмір кристалів $NiFe_2O_4$ близько 15 нм. Методом інфрачервоної спектроскопії з перетворенням Фур'є пояснено хімічні властивості $NiFe_2O_4$ коливаннями Fe–O. Досліджено магнітні властивості $NiFe_2O_4$, які корелюють з високою кристалічністю нанопластин $NiFe_2O_4$.

Феррит шпинели $NiFe_2O_4$ синтезирован низкотемпературным гидротермальным методом с различным соотношением $Ni(NO3)_2$ и $FeCl_2$, а именно 1:1, 1:2, 2:1 и 2:3, с последующим отжигом при температуре 300°C в течение 1 ч. Обнаружено, что формирование нанопластин происходит при низком содержании Ni и при более высоком содержании $FeCl_2$. Размер кристаллов $NiFe_2O_4$ порядка 15 нм. Методом инфракрасной спектроскопии с преобразованием Фурье объяснены химические свойства $NiFe_2O_4$ колебаниями Fe–O. Исследованы магнитные свойства $NiFe_2O_4$, которые коррелируют с высокой кристалличностью нанопластин $NiFe_2O_4$.

1. Introduction

In recent times, nanosized spinel ferrite particles have attracted considerable attention due to the enhancement of physical and chemical properties [1]. As an important member of the ferrite family, nickel ferrite ($NiFe_2O_4$) has attracted significant research interest because of its fascinating magnetic and electromagnetic properties [2]. $NiFe_2O_4$, an inverse spinel structure, shows ferromagnetism [3]. $NiFe_2O_4$ is a soft ferrite with low coercivity, high saturation mag-

netization, chemical stability and electrical resistivity, which makes it an excellent material for magnetic resonance imaging (MRI) enhancement, magnetic recording media and electronic devices [4, 5].

$NiFe_2O_4$ with typical ferromagnetic properties, low conductivity and stable thermal ability is suitable for a wide range of applications in many fields including gas sensors [6], microwave devices [7], data storage devices [8]. Nickel ferrite, with an inverse spinel structure, exhibits ferrimagnetism deriving from a magnetic moment of antiparallel spins between Fe^{3+} ions at tetrahedral sites and Ni^{2+} ions at octahedral sites.

Recently, many attempts have been made to synthesize various $NiFe_2O_4$ nanostructures in order to explore and enhance its properties and design the technological applications. 1D ferrite nanostructure can be synthesized by the sol-gel method, co-precipitation technique, microemulsion method, anodic aluminum oxide (AAO) template method, polymeric co-precipitation method and precursor method [9–11]. Among the many different synthesis methods, it is still extremely important to find simple and cost-effective routes for synthesizing nanocrystalline $NiFe_2O_4$ using cheap, non-toxic and environmentally friendly precursors. Hydrothermal synthesis of $NiFe_2O_4$ is a good technique for synthesis of the 1D nanostructure since it fulfils the above requirements [12, 13]. Self-assembly of the $NiFe_2O_4$ is achieved by introducing $FeCl_2$ and $Ni(NO_3)_2{\cdot}6H_2O$ precursors into the polymer, followed by co-precipitation. Single crystalline $NiFe_2O_4$ nanosheets are formed with the addition of urea (CH_4N_2O), which serves as a templating medium to form a crystalline $NiFe_2O_4$ nanosheet. The development of such mixed-$NiFe_2O_4$-based nanocomposites is aimed at functionalization in device technologies and optical applications.

2. Experimental

Synthesis of $NiFe_2O_4$ nanosheets

$Ni(NO_3)_2{\cdot}6H_2O$ (Merck, 99 %) and $FeCl_2$ (Merck, 99 %) with various ratios (1:1, 1:2, 2:1 and 2:3) were mixed into 50 mL deionized water through stirring and ultrasonication (Powersonic 600) for 15 min. The solution was then poured into a 100 ml Teflon-lined hydrothermal vessel heated to 200°C for 6 h. After cooled down to room temperature, the solution was precipitated by centrifugation at 4000 rpm for 5 min, followed by washing with distilled water and ethanol. The obtained powder was dried at 60°C in hotplate and further annealed at 300°C for 1 h in a furnace.

Field-emission scanning electron microscopy (FESEM) was carried out using a Hitachi SU-3500 instrument to determine the morphology of synthesized $NiFe_2O_4$. For analysis of microstructures of $NiFe_2O_4$, the X-ray diffraction (XRD) method (Rigaku Smartlab) was used with Cu–Kα (1.54 Å) radiation at diffraction angles from 10 to 80 deg. A Fourier-Transform Infrared Spectrometer (FTIR) (Thermo-Scientific Nicolet IS-10) was used to determine the chemical structure of $NiFe_2O_4$ by the KBr disk method with scanning in the range of 4000–450 cm^{-1}.

In order to investigate the magnetic properties of $NiFe_2O_4$, a vibrating sample magnetometer (VSM) VSM250 was used.

3. Results and discussion

Figure 1 shows the FESEM images of $NiFe_2O_4$ nanosheets with a small aggregation of primary $NiFe_2O_4$ nanoparticles, which causes the formation of sheet-like morphology. Although most of the nanosheets appear as separate, the surfaces are clearly not smooth, but contain some nanoparticles. It clearly indicates the initial stages for the growth of the nanosheets. For the $Ni(NO_3)_2$-to-$FeCl_2$ ratio of 1:1, Fig. 1a shows a clear evidence of nanosheets; but when the proportion of $Ni(NO_3)_2$ increases, the nanosheets become coarse with a rough surface (Fig. 1c). On the other hand, when the proportion of $FeCl_2$ increases to 1:2 and 2:3, the formation of nanoparticles becomes more dominant (Fig. 1b and d).

Fig. 2 shows powder XRD patterns of samples with various ratios between $Ni(NO_3)_2$ and $FeCl_2$. The peaks are indexed with an inverse spinel cubic phase with the space group of Fd3m, which is very well consistent with the JCPDS file (card no: 10-0325). In Fig. 2a, the pattern for $NiFe_2O_4$ at the $Ni(NO_3)_2$:$FeCl_2$ (1:1) ratio shows diffraction peaks at the angles of 18.4, 30.2, 35.6, 43.3, 53.7, 57.3 and 62.9 degrees, which can be indexed to (111) (220), (311), (400), (422), (511), (440) planes, respectively. For the (1:2) ratio, diffraction peaks at 18.4, 30.3, 35.6, 43.3, 53.8, 57.3 and 62.9 deg are revealed which can be indexed to (111) (220), (311), (400), (422), (511), (440) planes, respectively, as shown in Fig. 2b. For the (2:1) ratio, diffraction peaks at 18.4, 30.3, 35.6, 43.3, 53.8, 57.3 and 62.9 deg can be indexed to (111) (220), (311), (400), (422), (511), (440)

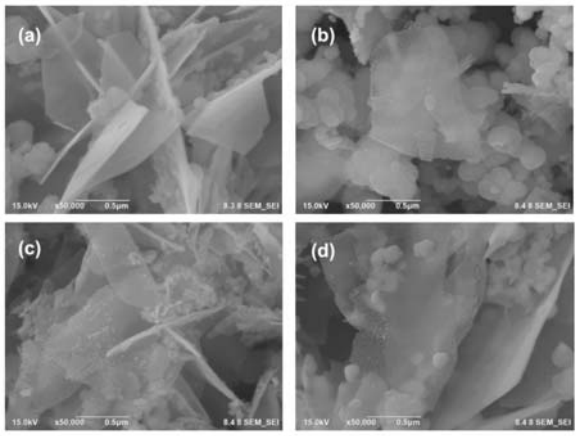

Fig. 1. FESEM images of $NiFe_2O_4$ with different ratios of $Ni(NO_3)_2$-to-$FeCl_2$ (a) 1:1, (b) 1:2, (c) 2:1 and (d) 2:3.

planes, respectively, as shown in Fig. 2c. And last, for the (2:3) ratio, diffraction peaks at 18.4, 30.3, 35.7, 43.4, 53.8, 57.3, and 63 deg can be indexed to (111) (220), (311), (400), (422), (511), (440) planes , respectively, as shown in Fig. 2d. The crystallite size of the $NiFe_2O_4$ phase is calculated using Scherrer's relation:

$$D = 0.9\lambda/\beta\cos\theta,$$

where β is the broadening of the diffraction line measured at half maximum intensity (radians); and $\lambda = 1.5406$ Å is the wavelength of CuKα. The average crystallite size for each 1:1, 1:2, 2:1 and 2:3 ratio is 10, 15, 8 and 15.8 nm, respectively.

The formation of the spinel structure in the synthesized $NiFe_2O_4$ sample was additionally confirmed by FT–IR spectrum as shown in Fig. 3. The band at 1090 cm^{-1} shows the presence of C–O group vibration modes. The band at 3394 cm^{-1} could be attributed to the O–H stretching vibration of H_2O absorbed by the sample and the surface O–H or EG. There is a significant change in the irrelevant peak of the C–H bending vibration band at 1697 cm^{-1}. The peaks at 1555 cm^{-1} are attributed to the N–O stretching vibration. The band at 594 cm^{-1} are assigned to the Fe–O tetrahedral site. The band at 2281 cm^{-1} shows the presence of the N=C=O stretching vibration. This results are in good accordance with the previous report [14].

The VSM analysis is the tool to investigate the magnetic properties of the prepared spinel ferrite samples. The room temperature VSM analysis was performed on

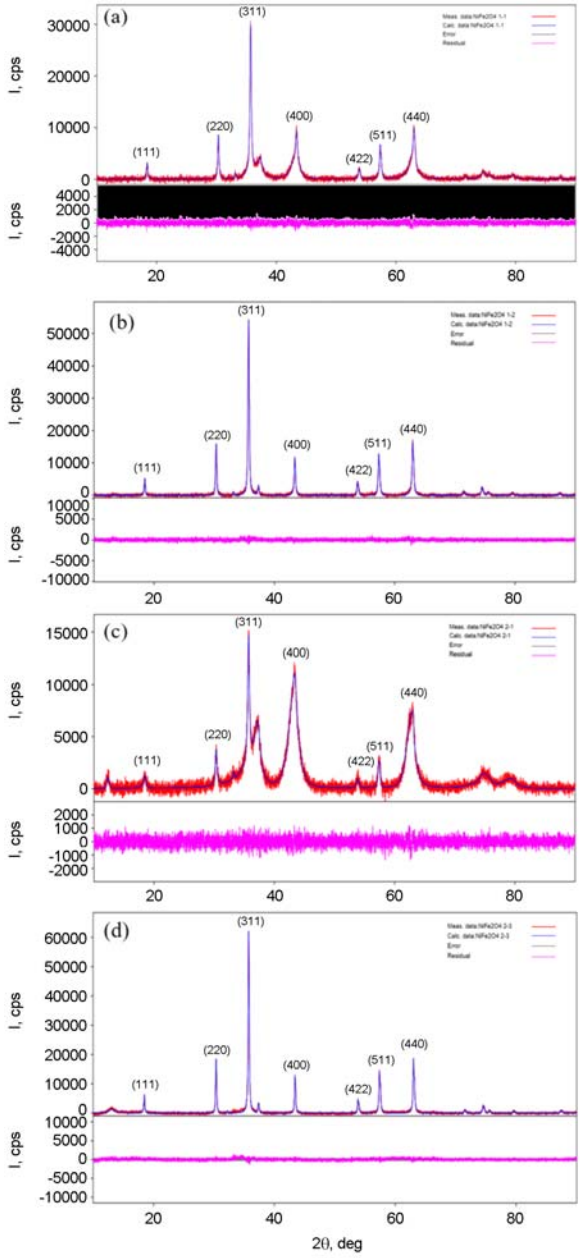

Fig. 2. XRD profile of $NiFe_2O_4$ with various ratios of $Ni(NO_3)_2$ to $FeCl_2$; (a) 1:1, (b) 1:2, (c) 2:1 and (d) 2:3.

$NiFe_2O_4$ nanosheets, and obtained magnetic hysteresis loops are shown in Fig. 4. The saturation magnetization (Ms), remanent magnetization (Mr), and coercivity (Hc) are 14.78 emu/g, 2.79 emu/g and 183.23 Oe, respectively, for the $Ni(NO_3)_2$:$FeCl_2$ (1:1) ratio; at the same time, for the ratio 2:1, Ms, Mr and Hc are 6.28 emu/g, 0.95 emu/g and 133.12 Oe, respectively. It is believed that the magnetic properties of materials depend on the shape of the sample, the direction of magnetization, crystallinity, etc.

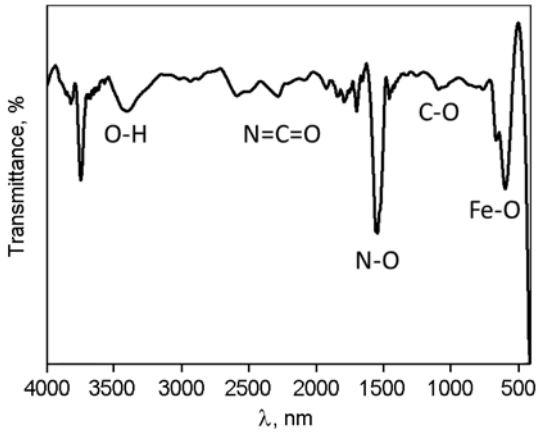

Fig. 3. FTIR analysis of $NiFe_2O_4$.

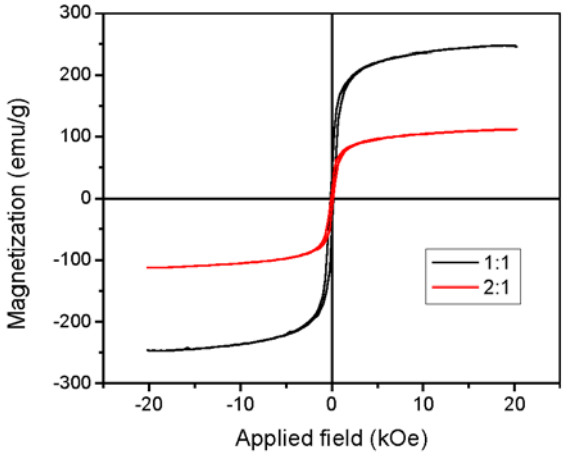

Fig. 4. Hysteresis loop for $NiFe_2O_4$ nanosheets: (a) $Ni(NO_3)_2$:$FeCl_2$ (1:1) and (b) $Ni(NO_3)_2$:$FeCl_2$ (2:1) at room temperature.

In the present work, nanosheets are formed through the agglomeration of magnetic nanoparticles; thus, the nanosheet sizes are closer to bulk. Therefore, their magnetic properties should be between those of the nanoparticles and the bulk material.

4. Conclusions

In summary, the $NiFe_2O_4$ nanosheets were successfully synthesized via facile hydrothermal methods with the addition of urea. According to FESEM images, the nanosheet structure was formed; however, with increasing Fe concentration, nanoparticles predominated in the structure of the nanosheets. The XRD analysis revealed the crystalline structure of $NiFe_2O_4$ at various $Ni(NO_3)_2$:$FeCl_2$ ratios with an average crystallite size of ~ 15 nm. FTIR results indicate the chemical structure of $NiFe_2O_4$ spinel ferrite. VSM shows that the magnetic properties of $NiFe_2O_4$ decrease with increasing Ni concentration.

Acknowledgements. The authors would like to thank Universitas Sumatera Utara Centre of Research for the financial support under contract No: 132/UN5.2.3.1/PPM/SPP-TALENTA USU/2020, 28 April 2020.

References

1. U.Luders, A.Barthelemy, M.Bibes et al., *Adv. Mater.*, **18**, 1733 (2006).
2. A.Ren, C.Liu, Y.Hong et al., *Chem. Eng. J.*, **258**, 301 (2014).
3. B.Palanivel, M.Shkir, T.Alshahrani, *Diamond Relat. Mater.*, **112**, 108148 (2020).
4. X.Shi, S.H.Wang, S.D.Swanson et al., *Adv. Mater.*, **20**, 1671 (2008).
5. J.Hong, D.Xu, J.Yu et al., *Nanotechnology*, **18**, 135608 (2007).
6. P.Lee, K.Ishizaka, H.Suematsu et al., *J. Nanopart. Res.*, **8**, 29 (2006).
7. A.More, V.Verenkar, S.Mojumdar et al., **94**, 63 (2008)
8. R.H.Kodama, A.E.Berkowitz, J.E.J.McNiff et al., *Phys. Rev. Lett.*, **77**, 394 (1996).
9. C.Thirupathy, S.C.Lims, S.J.Sundaram et al., *J. King Saud University-Sci.*, **32**, 1612 (2020).
10. L.Zhang, W.Jiao, *Sens. Actuat. B: Chem.*, **216**, 293 (2015).
11. M.George, A.M.John, S.S.Nair et al., *J. Magn. Magn. Mater.*, **302**, 190 (2006).
12. A.Baykal, N.Kasapoglu, Y.Koseoglu et al., *J. Alloys Compd.*, **464**, 514 (2008).
13. J.Zhou, J.Ma, C.Sun et al., *J. Am. Ceram. Soc.*, **88**, 3535 (2005).
14. P.Sivakumar, R.Ramesh, A.Ramanand et al., *Mater. Lett.*, **65**, 1438 (2011).